Babai-guided Interference-aware Adaptive QRD-M Detection in MIMO-OFDM Communication Systems

Mar Mar Lwin and Mohd Fadzli Mohd Salleh

Universiti Sains Malaysia, Nibong Tebal, Malaysia

https://doi.org/10.26636/jtit.2025.4.2290

Abstract — This paper presents an adaptive QRD-M detection algorithm designed to reduce the computational complexity of MIMO systems while maintaining near-maximum likelihood detection (near-MLD) performance. The proposed method introduces a dynamic threshold mechanism based on a breadth-first tree search, where pruning is guided by both symbol reliability and interlayer interference derived from the upper-triangular structure of the QR-decomposed channel matrix. The threshold is further refined using a Babai estimate obtained from Lenstra–Lenstra–Lovász (LLL) lattice reduction, allowing the algorithm to adaptively adjust the candidate set at each detection stage. The simulation results across 4 × 4 and 8 × 8 MIMO systems using 16-QAM and 64-QAM modulation schemes demonstrate that the proposed Babai-guided interference-aware adaptive QRD-M (BIA-QRD-M) algorithm achieves near-MLD performance. The proposed method achieves a reduction of up to 49% in the average number of branch metric computations at high SNR and an approximately 29% reduction over the entire 0 – 25 dB SNR range, compared to conventional QRD-M in an 8 × 8 MIMO-OFDM system with 16-QAM modulation.

Keywords — LLL lattice reduction, MIMO-OFDM systems, QRD-M detection

1. Introduction

Multiple input, multiple output (MIMO) systems are a key technology of high-capacity wireless communication solutions, offering substantial gains in spectral efficiency and link reliability. However, the associated symbol detection task becomes increasingly complex with high-order modulation and large antenna configurations. While maximum likelihood detection (MLD) [1] achieves optimal performance, it suffers from exponential grooving computational complexity, making it impractical for real-time implementations in most scenarios.

By contrast, linear detectors offer low implementation complexity but suffer from performance degradation under ill-conditioned channels. Lattice reduction preprocessing can partially mitigate this drawback [2]. To overcome this problem, a variety of suboptimal detection algorithms have been developed to approximate MLD with reduced complexity. Notable examples include sphere decoding (SD) [3], which performs an efficient search within a hypersphere, and the QRD-M algorithm [4], which limits the number of candidate paths retained during detection.

These methods aim to strike a balance between detection performance and computational feasibility, forming a basis for ongoing research into adaptive and low-complexity MIMO detection techniques.

Among these approaches, the QR decomposition with M algorithm (QRD-M) has gained popularity due to its structured tree search and consistent near-MLD performance. It first applies QR decomposition to the channel matrix and then selects M most reliable candidates at each detection layer based on the accumulated Euclidean distance. However, the algorithm still incurs high and fixed complexity, particularly when a large M is needed to maintain accuracy under high SNR or high-order modulation.

This paper addresses the performance-complexity trade-off in QRD-M, i.e. maintains near MLD performance while reducing the number of branch metric computations, using a Babai-guided, interference-aware adaptive threshold that scales with SNR.

2. Related Works

To address the computational burden of QRD-M, various improvements have been proposed. In [5], bounding techniques were applied to constrain the search region and reduce average complexity without significant performance degradation. In [6], an adaptive threshold was introduced in the K-best sphere decoding, dynamically adjusting the candidate list according to channel conditions. Within the QRD-M framework, path elimination is pruned. This approach offers complexity savings that are inherently dependent on the modulation method proposed in [7], where branches with accumulated Euclidean distances exceeding the minimum at each layer are of order.

In [8], a Babai-based thresholding approach was proposed, where the candidate set is adaptively expanded when initial pruning yields too few surviving paths. This method achieves lower average complexity in many scenarios by combining aggressive pruning with selective recovery of candidates. However, its dynamic expansion behavior can introduce vari-

ability in computational load and requires careful threshold tuning.

In [9], the set was restricted to a modulation-specific neighborhood centered around a QR-based estimate. While this approach effectively reduces complexity, it lacks adaptability across different modulation formats and does not account for inter-layer interference or symbol reliability. The radius of the neighborhood is manually configured per modulation format, limiting the flexibility in heterogeneous or dynamically varying scenarios.

These limitations highlight the need for a more general pruning strategy that takes advantage of standard preprocessing, avoids heuristic dependencies, and adapts reliably to varying MIMO-OFDM configurations. Such trade-offs described across prior works motivate the development of a pruning method that offers adaptively bounded complexity across SNR regimes and system configurations, without reliance on modulation-specific thresholds.

Despite these efforts, achieving near-MLD performance with low complexity and without relying on modulation-specific structures or heuristics remains an open challenge. This paper proposes an adaptive pruning strategy based on interference-aware thresholding, which dynamically adjusts the candidate set using symbol reliability and channel structure, and does so without relying on modulation-specific heuristics.

Complementary research investigates iterative detectors aided by lattice reduction [10] and model driven deep learning detectors [11]. These approaches typically require soft information exchange or offline training, whereas the present study advances the hard decision QRD-M family with a training-free, rule-based threshold that directly reduces branch metric (SED) counts.

Here, a Babai-guided, interference-aware adaptive threshold with SNR dependent scaling is introduced for QRD-M to adjust the survivor set per layer without training or soft output. The algorithm integrates the deviation from the Babai point with a normalized interlayer interference term derived from the upper triangular matrix, thereby stabilizing pruning across SNR regimes and channel conditions. The resulting detector reduces branch metric (SED) counts while preserving near MLD performance, and is validated on 4 × 4 and 8 × 8 MIMO-OFDM with 16-QAM and 64-QAM under flat and frequency selective channels.

3. System Description

A spatial multiplexing multiple input multiple output (MIMO) system is modeled with N_T transmit antennas and N_R receive antennas, under the assumption that $N_R \geqslant N_T$. The received signal vector $\boldsymbol{y} \in \mathbb{C}^{N_R}$ is given by [12]:

$$\boldsymbol{y} = \mathbf{H}\boldsymbol{x} + \boldsymbol{n}\,, \tag{1}$$

where $\mathbf{H} \in \mathbb{C}^{N_R \times N_T}$ denotes the complex-valued flat fading channel matrix, the transmitted symbol vector $\boldsymbol{x} \in S^{N_T}$ is drawn from a constellation set S, such as QAM or PAM, and $\boldsymbol{n} \sim \mathcal{CN}(0, \sigma^2 \mathbf{I}_{N_R})$ is additive white Gaussian noise with variance σ^2.

To enable efficient detection, QR decomposition is applied to channel matrix $\mathbf{H}$, yielding the following:

$$\mathbf{H} = \mathbf{QR}\,, \tag{2}$$

where $\mathbf{Q} \in \mathbb{C}^{N_R \times N_T}$ is a unitary matrix (i.e. $\mathbf{Q}^H\mathbf{Q} = \mathbf{I}_{N_T}$) and $\mathbf{R} \in \mathbb{C}^{N_T \times N_T}$ is an upper-triangular matrix.

Multiplying both sides of Eq. (1) by $\mathbf{Q}^H$ results in an upper-triangular form:

$$\hat{\boldsymbol{y}} = \mathbf{Q}^H\boldsymbol{y} = \mathbf{R}\boldsymbol{x} + \hat{\boldsymbol{n}}\,. \tag{3}$$

Here, $\hat{\boldsymbol{y}} \in \mathbb{C}^{N_R}$ is the transformed received vector and $\hat{\boldsymbol{n}} = \mathbf{Q}^H\boldsymbol{n}$ retains the same statistical properties due to the unitary nature of $\mathbf{Q}$.

Based on the triangular system model, the goal of MIMO detection is to estimate the vector of the transmitted symbol vector $\boldsymbol{x} \in S^{N_T}$ from the transformed observation $\hat{\boldsymbol{y}} = \mathbf{Q}^H\boldsymbol{y}$. This is achieved by finding the vector that minimizes the discrepancy between the received signal and its reconstruction through the channel. Mathematically, the detection task is formulated as an integer least squares (ILS) problem given by:

$$\hat{\boldsymbol{x}} = \arg \min_{\boldsymbol{x} \in S^{N_T}} \|\hat{\boldsymbol{y}} - \mathbf{R}\boldsymbol{x}\|^2\,, \tag{4}$$

where $\mathbf{R}$ is the upper-triangular matrix obtained from QR decomposition. Solution $\hat{\boldsymbol{x}}$ represents the closest point in the lattice generated by $\mathbf{R}$ to observation $\hat{\boldsymbol{y}}$, under the constraint that the components of $\boldsymbol{x}$ are drawn from a discrete modulation set S.

Solving this problem exactly yields the maximum likelihood (ML) estimate, but its computational complexity grows exponentially with N_T and the constellation size. Therefore, suboptimal but efficient detection algorithms such as SD and QRD-M are typically used to approximate the ML solution.

3.1. QRD-M Detection

QRD-M is a breadth-first tree search algorithm designed to approximate the solution of the integer least squares (ILS) problem defined in Eq. (4), based on the representation of the triangular system in Eq. (3). The detection objective is to find that the transmitted vector $\boldsymbol{x} \in S^{N_T}$ minimizes the squared Euclidean distance between the transformed received signal $\hat{\boldsymbol{y}}$ and its reconstruction via the upper-triangular matrix $\mathbf{R}$.

The squared Euclidean distance (SED) is given by:

$$\text{SED} = \|\hat{\boldsymbol{y}} - \mathbf{R}\boldsymbol{x}\|^2\,. \tag{5}$$

Because $\mathbf{R}$ is upper-triangular, each component of the residual depends only on $\boldsymbol{x}_1, \ldots, \boldsymbol{x}_{N_T}$. Hence Eq. (5) can be written as:

$$\|\hat{\boldsymbol{y}} - \mathbf{R}\boldsymbol{x}\|^2 = \sum_{i=1}^{N_T} \left\| \hat{\boldsymbol{y}}_i - \sum_{j=i}^{N_T} \mathbf{R}_{ij}\boldsymbol{x}_j \right\|^2\,, \tag{6}$$

where $\mathbf{R}_{ij}$ denotes the element in the i-th row and j-th column of matrix $\mathbf{R}$, $\hat{\boldsymbol{y}}_i$ is the i-th received signal after nulling and $\boldsymbol{x}_j$ is the j-th transmit signal.

This layer-wise expansion reveals the interference structure embedded in each received component $\hat{\boldsymbol{y}}_i$. Specifically, the term $\sum_{j=i}^{N_T} \mathbf{R}_{ij}\, \boldsymbol{x}_j$ represents inter-layer interference from symbols $\boldsymbol{x}_j$ not yet decided in the detection process. As detection progresses from stage $i = N_T$ (root node) to stage $i = 1$ (first layer), the interference accumulates and becomes more significant, particularly in ill-conditioned channels.

The conventional QRD-M algorithm mitigates this by maintaining a fixed number M of candidate paths at each stage, selecting the highest M symbol extensions with the smallest partial Euclidean distance. Although conventional QRD-M provides a computationally efficient approximation to maximum likelihood detection, its fixed candidate size does not respond to variations in interference or noise conditions. This limitation motivates the development of an adaptive approach.

3.2. Proposed Method

The proposed Babai-guided interference-aware adaptive QRD-M (BIA-QRD-M) algorithm enhances the conventional QRD-M by adaptively pruning symbol candidates at each detection layer based on the local structure of the received signal. Unlike fixed m QRD-M, which retains a constant number of candidates regardless of channel or noise conditions, BIA-QRD-M dynamically adjusts the pruning threshold using a combination of Babai point deviation and a normalized interference plus noise term, both computed from the QR decomposition of the LLL-reduced basis channel matrix. This integration of lattice reduction enhances orthogonality and improves the reliability of the Babai estimate used for adaptive pruning.

The QRD-M algorithm improves detection accuracy over linear detectors by exploring multiple symbol candidates at each detection layer. However, the fixed-M QRD-M expands a predetermined number of candidates regardless of signal quality or interference level, resulting in either excessive complexity or insufficient accuracy.

To address this, an adaptive pruning strategy is proposed that dynamically adjusts the number of candidates in each layer based on symbol reliability and the magnitude. At each detection layer i, the pruning threshold η_i determines the allowable deviation from the Babai estimate, taking into account both symbol reliability and the impact of interlayer interference.

The threshold at layer i is defined as:

$$\eta_i = \frac{\gamma \cdot |\hat{\boldsymbol{b}}_i - \widetilde{\boldsymbol{y}}_i| + \delta \cdot \left(\frac{\sum_{j=i+1}^{N_T} \left|\widetilde{\mathbf{R}}_{i,j}\right|}{\left|\widetilde{\mathbf{R}}_{i,i}\right|} \right)}{1 + \alpha \cdot SNR_{\text{linear}}}, \tag{7}$$

where:

- $\widetilde{\mathbf{Q}}$ and $\widetilde{\mathbf{R}}$ are LLL-reduced basis obtained from the complex-valued channel matrix $\mathbf{H}$, while $\widetilde{\mathbf{R}}_{i,j}$ are entries of the upper-triangular matrix $\widetilde{\mathbf{R}}$,
- $\hat{\boldsymbol{b}}_i$ is the Babai estimate at layer i, calculated from the ZF solution $\hat{\boldsymbol{x}}_{ZF} = \widetilde{\mathbf{R}}^{-1}\hat{\boldsymbol{b}}_i$, followed by nearest neighbour rounding,
- $\widetilde{\boldsymbol{y}}_i = [\widetilde{\mathbf{Q}}^H \boldsymbol{y}]_i$ is the i-th component of the transformed received vector,
- $\gamma > 0$ and $\delta > 0$ are user-defined parameters,
- $\alpha \geqslant 0$ is a scaling parameter that adjusts the overall pruning aggressiveness with respect to SNR, ensuring that the threshold becomes tighter at high SNR and looser at low SNR,
- $SNR_{\text{linear}} = 10^{\frac{SNR_{dB}}{10}}$ converts the SNR value from decibels to a linear scale.

For all simulations, $\alpha = 0.5$ is used for a flat-fading channel, while $\alpha = 0.02$ is applied to frequency-selective fading channels. Parameters γ and δ are fixed at 1.5 and 2.0, respectively, in all scenarios.

In contrast to fixed thresholds based on Babai or neighborhood margins, the proposed scheme determines the pruning level from the deviation to the Babai point, together with a normalized measure of interlayer interference computed from the upper-triangular factor of the QR decomposition, with explicit SNR dependent scaling. This rule-based, layer adaptive mechanism reduces branch metric (SED) counts while maintaining near-MLD candidates.

This formulation incorporates three key observations:

1. **Symbol reliability.** The term $|\hat{\boldsymbol{b}}_i - \widetilde{\boldsymbol{y}}_i|$ quantifies the deviation between the Babai estimate and the transformed received symbol in the LLL-reduced domain. A smaller value indicates that the Babai estimate closely aligns with the underlying received symbol, suggesting high confidence in rounding decision and allowing for tighter pruning.

2. **Normalized interference term.** The summation $\sum_{j=i+1}^{N_T} \left|\widetilde{\mathbf{R}}_{i,j}\right|$ captures the cumulative effect of undecided symbols from lower layers. Dividing this by the diagonal term $\left|\widetilde{\mathbf{R}}_{i,i}\right|$ normalizes the interference with respect to the signal strength at the current layer. A higher normalized value implies stronger residual interference, prompting looser pruning to maintain detection robustness.

3. **SNR-dependent scaling.** The denominator term $1 + \alpha \cdot SNR_{\text{linear}}$ introduces a global control mechanism that tightens the threshold as the signal-to-noise ratio increases. At high SNR, where symbol estimates become more reliable, the threshold becomes smaller, enabling more aggressive pruning. At low SNR, the threshold is relaxed, ensuring robustness under noise-dominant conditions.

Together, these three components allow the threshold to dynamically adapt based on both local layer conditions (symbol confidence and interference) and global channel reliability (SNR). This adaptive mechanism balances detection performance and computational complexity more effectively than fixed-M approaches.

Parameters γ, δ, and α serve as tuning knobs operating in the following manner:

- Increasing γ makes the pruning more sensitive to the Babai point error, emphasizing symbol reliability,
- Increasing δ gives more weight to normalized interference, relaxing the threshold in high interference layers,
- Increasing α intensifies the influence of SNR, imposing a tighter threshold as channel conditions improve.

This design ensures that a larger number of candidates is evaluated only when necessary, achieving near-optimal detection performance while significantly reducing average complexity across a wide range of SNR and channel conditions.

The detection procedure is as follows:

Initialization. The detection process begins by applying the QR decomposition to the channel matrix and transforming the received vector accordingly.

Candidate evaluation and metric computation. Starting from the N_T-th layer, all constellation symbols are considered as candidates. For each candidate, the squared Euclidean distance (branch metric) is computed relative to the transformed received signal and the upper-triangular matrix.

Adaptive thresholding and pruning. Once the branch metrics are computed, a dynamic threshold η_i is calculated at each layer to eliminate the unlikely candidates. The proposed threshold formulation incorporates three components: the mismatch between the Babai point and the transformed received symbol, a normalized interference term derived from the structure of the upper triangular matrix, and an SNR-dependent denominator that adaptively tightens the threshold magnitude under high SNR conditions. Complex LLL reduction is applied locally within the threshold computation to improve pruning reliability. Symbol candidates with branch metrics exceeding η_i are pruned. This process is repeated from layer N_T down to layer 1.

Path selection. After pruning is applied to layer N_T down to layer 1, each surviving path corresponds to a complete symbol vector. Among these, the candidate with the lowest branch metric in layer 1 is selected as the final estimate, and the corresponding symbol vector is reconstructed by tracking the selected path.

The pseudocode presented as Algorithm 1 describes the detection procedure with adaptive pruning applied at each layer. Branch metrics are computed for candidate symbols and compared against a dynamic threshold which has been derived from the Babai point, the upper triangular matrix, and the SNR. This selective pruning reduces computational complexity by eliminating unlikely candidates early in the search.

The proposed algorithm dynamically adjusts the number of candidates at each detection layer based on a symbol-wise reliability metric and an interference-sensitive threshold. The threshold formulation incorporates SNR normalization, enabling the algorithm to prune the candidate paths more aggressively when the symbol estimate is deemed highly reliable and to retain more paths when uncertainty is greater. This adaptive mechanism achieves a favorable balance between detection performance and computational complexity.

3.3. Complexity Analysis

Computational complexity in MIMO detection algorithms can be evaluated using different metrics, such as execution time (latency) or analytical expressions like Big-$\mathcal{O}$ notation. In this work, complexity is quantified in terms of the number of SED computations, which directly reflects the effort required in evaluating candidates during detection. This metric provides a practical measure of computational load and allows meaningful comparison between different detection schemes from a simulation-based perspective.

In this work, complexity is reported as the number of SED evaluations. Each SED evaluation represents a metric computation triggered by the expansion of the candidate and reflects the actual search workload. Because it is independent of the computing platform and memory configuration, the SED count provides a consistent indicator of computational demand and is therefore more reliable than runtime measurements, which can vary with simulation environment and system resources.

In ML and near-ML detections, the primary contributor to computational complexity is the repeated evaluation of SEDs derived from the ILS equation. The complexity of the proposed method is expressed in terms of total SED calculations and compared with conventional QRD-M detection, forming a basis for the subsequent performance–complexity trade-off analysis.

4. Results and Discussion

This section presents the symbol error rate (SER) performance and computational complexity of the proposed adaptive QRD-M detection method. Simulation results are provided to evaluate the method under various MIMO configurations and modulation schemes. Performance benchmarking includes sphere decoding (SD) for SER only, while both performance and complexity are compared against conventional QRD-M to isolate the effect of the proposed adaptive threshold.

Particular attention is given to the impact of the adaptive threshold on pruning behavior and its influence on performance across different SNR values. Table 1 lists the core simulation parameters used in the performance evaluation and complexity analysis.

Figure 1 illustrates SER performance of conventional QRD-M detection compared to SD in a 4 × 4 MIMO system with 8-PAM modulation. The SD curve, adapted from [13], represents near-ML performance. With increasing M, QRD-M approaches SD. At maximum list size $M = 8$, QRD-M is equivalent to SD (near-ML) reference. This demonstrates that a sufficiently large M enables QRD-M to approximate ML accuracy. In contrast, lower values (e.g. $M = 4$) show noticeable performance degradation at higher SNRs. This comparison validates the use of SD as a reference to assess the effectiveness of suboptimal detection algorithms.

Figure 2 presents SER performance of the proposed BIA-QRD-M method compared to conventional QRD-M with fixed M values of 8, 12, and 16 in a 4 × 4 MIMO system using

Algorithm 1 Pseudocode for the proposed BIA-QRD-M

Input: $H, y, PAM_{table}, M_{init}, M_{min}, \gamma, \delta, \alpha$
Output: estimated symbol vector $\hat{x}$

$[Q, R] = \mathrm{QR}(H)$ ▷ QR decomposition for detection
$\hat{y} = Q^H y$ ▷ Transformed received vector for metric computation
$[\tilde{Q}, \tilde{R}, T] = \mathrm{LLL}(H)$ ▷ Complex LLL for threshold computation
$\tilde{y} = \tilde{Q}^H y$ ▷ Transformed received vector for threshold computation
Step 1: Root layer (layer N_T)
for each symbol x in the `PAM_table` **do**
  Initialize path with symbol x at layer N_T
  $d_i = |\hat{y}_{N_T} - R_{N_T,N_T} x|^2$ ▷ Compute branch metric
  $\hat{b} = \mathrm{round}\left(\frac{\tilde{y}_{N_T}}{\tilde{R}_{N_T,N_T}}\right)$ ▷ Babai estimate
  $interference = 0$
  $\eta_i = \frac{\gamma\,|\hat{b} - \tilde{y}_{N_T}| + \delta\, interference}{1 + \alpha\, SNR_{linear}}$ ▷ Threshold
  if $d_i \leqslant \eta_i$ **then**
    Add candidate to `surviving_paths`
  end if
  if $\mathrm{length}(\texttt{surviving\_paths}) < M_{min}$ **then**
    $M = M_{min}$
  else $M = \mathrm{length}(\texttt{surviving\_paths})$
  end if
  Store the top M surviving candidates for extension at the next layer
end for
Step 2: Remaining layers (from $N_T - 1$ to 1)
for layer = $N_T - 1$ down to 1 **do**
  for each extended candidate ($x \in$ `PAM_table`) from layer $+1$ **do**
    $\textit{contribution\_from\_lower\_layers} = \sum_{j=layer+1}^{N_T} R_{layer,j} \hat{x}_j$
    $d_i = |\, \hat{y}_{\text{layer}} - R_{\text{layer,layer}} x_{\text{layer}} - \textit{contribution\_from\_lower\_layers}\,|^2$
    $\textit{babai\_term} = \sum_{j=\text{layer}+1}^{N_T} \tilde{R}_{\text{layer},j}\, \hat{x}_j$
    $\hat{b} = \mathrm{round}\left(\frac{\tilde{y}_{\text{layer}} - \textit{babai\_term}}{\tilde{R}_{\text{layer, layer}}}\right)$
    $\textit{interference} = \frac{\sum_{j=\text{layer}+1}^{N_T} \left|\tilde{R}_{\text{layer},j}\right|}{\left|\tilde{R}_{\text{layer, layer}}\right|}$
    $\eta_i = \frac{\gamma\,|\hat{b} - \tilde{y}_{\text{layer}}| + \delta\, interference}{1 + \alpha\, SNR_{linear}}$ ▷ Threshold
    if $d_i \leqslant \eta_i$ **then**
      Add candidate to `surviving_paths`
      if $\mathrm{length}(\texttt{surviving\_paths}) < M_{min}$ **then**
        $M = M_{min}$
      else
        $M = \mathrm{length}(\texttt{surviving\_paths})$
      end if
    end if
  end for
  Store the top M surviving candidates for extension at the next layer
end for
Step 3: Final decision
At layer 1, select the candidate with the minimum branch metric
Reconstruct the full symbol vector $\hat{x}$ from the selected path
Return $\hat{x}$
End

Tab. 1. Simulation parameters.

Parameter	Value
No. of subcarries (FFT size)	64
OFDM symbols per frame	14, used only for Monte Carlo averaging, not per-symbol detection
Channel model	Rayleigh flat-fading (1 tap i.i.d.) and frequency-selective (5 taps, Rayleigh fading with exponential power-delay profile)
Number of channel taps	5
Modulation scheme	16-QAM, 64-QAM
MIMO system	4 × 4, 8 × 8
Detection methods	Conventional QRD-M, proposed BIA-QRD-M

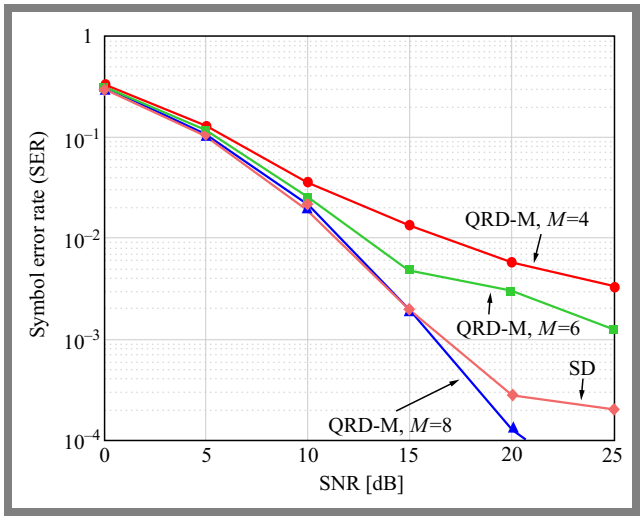

Fig. 1. Comparison of QRD-M detection with M = 4, 6, and 8, and SD in a 4 × 4 MIMO system using 8-PAM modulation.

16-QAM modulation. A larger M in QRD-M detection generally improves accuracy by retaining more candidate paths. In this 16-QAM scenario, the proposed method achieves SER performance that closely matches that of conventional QRD-M with $M = 12$. This demonstrates that the proposed approach achieves near-optimal detection performance while significantly reducing computational complexity, particularly in the medium-to-high SNR regime.

Figure 3 illustrates SER versus SNR for various MIMO configurations and modulation schemes of the proposed BIA-QRD-M system. As shown in Fig. 3, the 4 × 4 MIMO system employing 64-QAM achieves superior SER performance compared to the 4 × 4 MIMO system with 16-QAM, highlighting the advantage of higher-order modulation in terms of detection accuracy.

However, this improvement comes at the expense of increased computational complexity (see subsequent results). Furthermore, comparing 16-QAM, the 8 × 8 MIMO demonstrates enhanced SER performance due to the increased spatial diversity, although with a significantly higher computational cost.

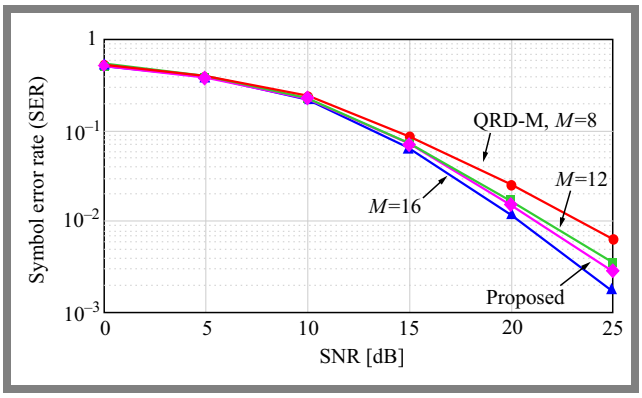

Fig. 2. SER of conventional QRD-M detection with M = 8, 12, and 16, versus the proposed method in a 4 × 4 MIMO system using 16-QAM modulation.

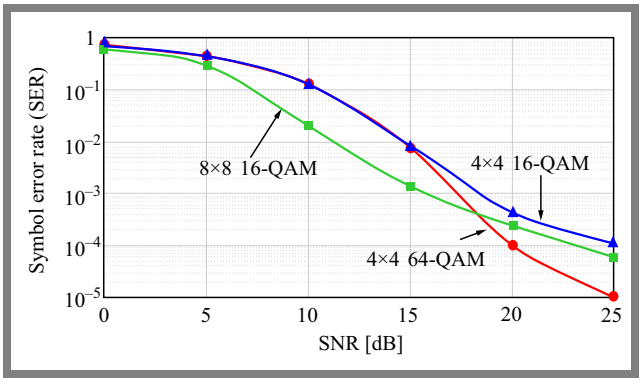

Fig. 3. SER performance of the proposed BIA-QRD-M detection method for 4 × 4 and 8 × 8 MIMO-OFDM systems using 16-QAM and 64-QAM modulation schemes over a flat-fading channel.

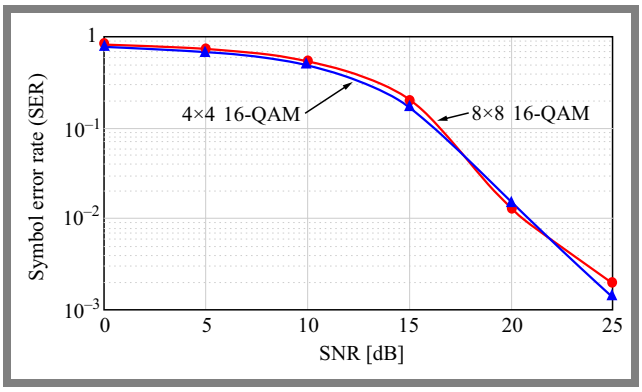

Fig. 4. SER performance of the proposed BIA-QRD-M detection method for 4 × 4 and 8 × 8 MIMO-OFDM systems using 16-QAM modulation over a frequency-selective fading channel.

Figure 4 shows SER performance of the proposed BIA-QAD-M detection method for 4 × 4 and 8 × 8 MIMO-OFDM systems over frequency-selective Rayleigh fading channels. In both configurations, SER decreases consistently with increasing SNR, showing that the proposed method maintains reliable detection accuracy across a wide SNR range.

Following the analysis of the symbol error rate performance, the subsequent focus is on computational complexity. The

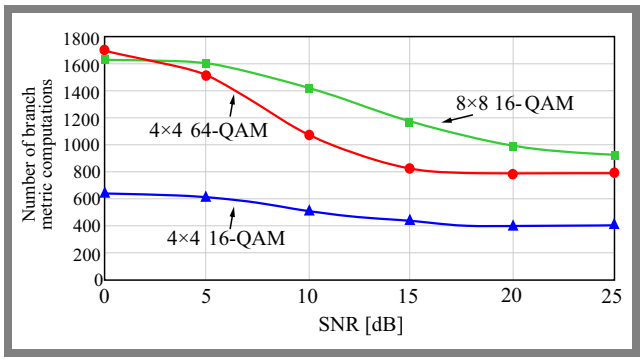

Fig. 5. Average number of branch-metric computations per detection versus SNR for the proposed BIA-QRD-M algorithm in 4 × 4 and 8 × 8 MIMO-OFDM systems using 16-QAM and 64-QAM modulation schemes over a flat-fading channel.

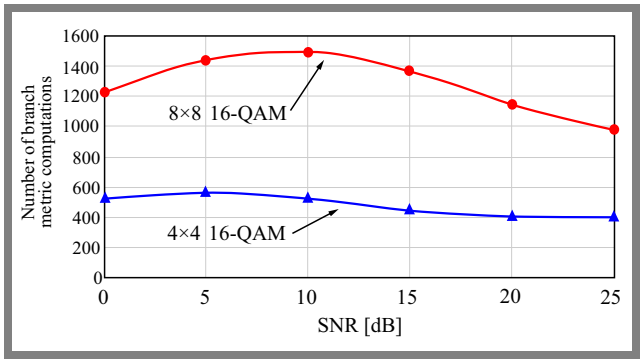

Fig. 6. Average number of branch-metric computations per detection versus SNR for the proposed BIA-QRD-M algorithm in a 4 × 4 and 8 × 8 MIMO-OFDM systems using 16-QAM modulation over a frequency-selective fading channel.

computational cost of the proposed BIA-QRD-M detection algorithm is evaluated under various modulation schemes and MIMO configurations, measured in terms of the average number of branch-metric computations.

The average number of branch metric computations as a function of SNR for the proposed method in 4 × 4 and 8 × 8 MIMO systems using 16-QAM and 64-QAM modulation schemes is presented in Fig. 5. As expected, the computational complexity increases with modulation order. The results confirm that both higher-order modulation and increased antenna count lead to higher computational demands, which is consistent with theoretical expectations.

Figure 6 presents a complexity analysis of the proposed BIA-QRD-M detection method for 4 × 4 and 8 × 8 MIMO-OFDM systems under frequency-selective fading conditions. The results show that the proposed method achieves a substantial reduction in the average number of branch metric computations compared with the conventional QRD-M approach, particularly in the high-SNR region. This reduction is more pronounced for the frequency selective channel due to the enhanced pruning effectiveness at higher SNR, confirming the method's ability to maintain detection accuracy while significantly lowering computational requirements.

A comparison of the average number of branch-metric computations for the proposed method with conventional QRD-M detection using fixed m values of 8, 12, and 16 in a 4 × 4 MIMO system with 16-QAM modulation is illustrated in Fig. 7. Although conventional QRD-M exhibits constant complexity regardless of SNR, the proposed method demonstrates a clear SNR-dependent reduction in computational cost. At high SNR levels, the proposed method approaches the complexity of QRD-M with $M = 8$, the lowest fixed setting, while at low SNR, it maintains a complexity level below that of QRD-M with $M = 12$. This adaptive behavior enables significant complexity savings while preserving detection performance, making it especially attractive for scenarios with dynamic channel conditions.

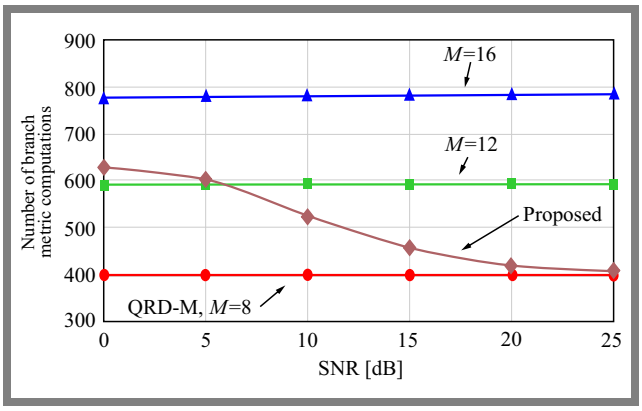

Fig. 7. Comparison of the average number of branch metric computations of conventional QRD-M detection with M = 8, 12, 16, and the proposed method in a 4 × 4 MIMO system with 16-QAM.

To summarize the performance–complexity trade-off, see Tab. 2 presenting a comparative analysis of the proposed and conventional QRD-M methods under various MIMO configurations and modulation schemes at low (10 dB), moderate (15 dB), and high (25 dB) SNR levels. Under 16-QAM modulation, the proposed method consistently outperforms the conventional QRD-M in both 4 × 4 and 8 × 8 MIMO settings. At 10 dB, the 4 × 4 system achieves a lower SER (0.1214 vs. 0.1341) while reducing the branch metric count by more than 20% (424 vs. 541). This efficiency becomes more prominent at 15 dB and 25 dB, where the proposed algorithm cuts complexity by nearly 50% in the 4 × 4 case and by more than 35% in the 8 × 8 case, without compromising SER performance.

For 64-QAM modulation in the 4 × 4 configuration, the trade-off becomes even more evident. At 10 dB, the proposed method significantly reduces SER (0.1250 vs. 0.5697) while requiring only 8.5% of the metric computations (1068 vs. 12 508), indicating substantial gains in both accuracy and efficiency. These benefits are maintained at higher SNR levels. At 15 dB, the SER drops below 10^{-3} with only 818 metric evaluations, i.e. far below the conventional method's complexity threshold.

Across all scenarios shown in Tab. 2, the proposed interference-sensitive pruning strategy enables scalable complexity control while maintaining high detection accuracy. The improvements are particularly pronounced under high-order modulation and larger MIMO sizes, confirming effectiveness in the performance-complexity trade-off for MIMO-OFDM systems.

Tab. 2. Performance–complexity trade-off of conventional and proposed QRD-M detection methods under various MIMO configurations and modulation schemes.

SNR [dB]	MIMO	Modulation	Complexity (QRD-M)	Complexity (proposed)	SER (QRD-M)	SER (proposed)
10	4 × 4	16-QAM	784	518	0.222	0.1315
15	4 × 4	16-QAM	784	425	0.07625	8.398×10^{-3}
25	4 × 4	16-QAM	784	400	2.75×10^{-3}	1.116×10^{-4}
10	4 × 4	64-QAM	12 352	1068	0.5697	0.1250
15	4 × 4	64-QAM	12 352	818	0.3725	0.0079
25	4 × 4	64-QAM	12 352	784	0.0295	0
10	8 × 8	16-QAM	1808	1420	0.1003	0.01965
15	8 × 8	16-QAM	1808	1163	0.0115	0.0013
25	8 × 8	16-QAM	1808	923	8.75×10^{-4}	5.859×10^{-5}

5. Conclusions

This paper presents an adaptive QRD-M detection algorithm enhanced by an interference-aware pruning strategy, designed for scalable and efficient MIMO-OFDM systems. By dynamically adjusting the candidate set based on symbol reliability and inter-layer interference, the proposed method reduces computational complexity while maintaining near-MLD performance. Unlike previous approaches that rely on fixed m configurations, modulation-specific heuristics, or noise-dependent tuning, the proposed scheme adapts to the detection structure itself, ensuring robustness across a wide range of MIMO sizes and modulation formats. The simulation results confirmed that the proposed method improves both detection accuracy and computational efficiency, especially in large-scale and high-order MIMO settings.

These results affirm the practicality for modern wireless systems that require high spectral efficiency under constrained computational resources. This paper reports evaluations for 4 × 4 and 8 × 8 configurations, reflecting the scope commonly adopted in non-linear MIMO detection studies.

References

[1] K. Miura, "An Introduction to Maximum Likelihood Estimation and Information Geometry", *Interdisciplinary Information Sciences*, vol. 17, pp. 155–174, 2011 (https://doi.org/10.4036/iis.2011.155).

[2] Q. Zhou and X. Ma, "Element-based Lattice Reduction Algorithms for Large MIMO Detection", *IEEE Journal on Selected Areas in Communications*, vol. 31, pp. 274–286, 2013 (https://doi.org/10.1109/JSAC.2013.130215).

[3] M.O. Damen, H. El Gamal, and G. Caire, "On Maximum-likelihood Detection and the Search for the Closest Lattice Point", *IEEE Transactions on Information Theory*, vol. 49, pp. 2389–2402, 2003 (https://doi.org/10.1109/TIT.2003.817444).

[4] W.H. Chin, "QRD Based Tree Search Data Detection for MIMO Communication Systems", *2005 IEEE 61st Vehicular Technology Conference*, Stockholm, Sweden, 2005 (https://doi.org/10.1109/VETECS.2005.1543595).

[5] M. Mohaisen and K. Chang, "Upper-lower Bounded-complexity QRD-M for Spatial Multiplexing MIMO-OFDM Systems", *Wireless Personal Communications*, vol. 61, pp. 129–141, 2011 (https://doi.org/10.1007/s11277-010-0014-8).

[6] U. Ummatov and K. Lee, "Adaptive Threshold-aided K-best Sphere Decoding for Large MIMO Systems", *Applied Sciences*, vol. 9, art. no. 4624, 2019 (https://doi.org/10.3390/app9214624).

[7] J.-H. Ro, J.-K. Kim, Y.-H. You, and H.-K. Song, "Low-complexity QRD-M with Path Eliminations in MIMO-OFDM Systems", *Applied Sciences*, vol. 7, art. no. 1206, 2017 (https://doi.org/10.3390/app7121206).

[8] S.-J. Choi *et al.*, "Novel MIMO Detection with Improved Complexity for Near-ML Detection in MIMO-OFDM Systems", *IEEE Access*, vol. 7, pp. 60389–60398, 2019 (https://doi.org/10.1109/ACCESS.2019.2914707).

[9] B.S. Kim, S.D. Kim, D. Na, and K. Choi, "A Very Low Complexity QRD-M MIMO Detection Based on Adaptive Search Area", *Electronics*, vol. 9, art. no. 756, 2020 (https://doi.org/10.3390/electronics9050756).

[10] H. Liu *et al.*, "A Novel Iterative Detection Method Based on a Lattice Reduction-aided Algorithm for MIMO OFDM Systems", *Scientific Reports*, vol. 14, art. no. 2779, 2024 (https://doi.org/10.1038/s41598-024-52602-6).

[11] X. Zhou *et al.*, "Model-driven Deep Learning-based MIMO-OFDM Detector: Design, Simulation, and Experimental Results", *IEEE Transactions on Communications*, vol. 70, pp. 5193–5207, 2022 (https://doi.org/10.1109/TCOMM.2022.3186404).

[12] T.-D. Chiueh, P.-Y. Tsai, and I.-W. Lai, *Baseband Receiver Design for Wireless MIMO-OFDM Communications*, Wiley, 346 p., 2012 (https://doi.org/10.1002/9781118188194).

[13] A. Ghasemmehdi and E. Agrell, "Faster Recursions in Sphere Decoding", *IEEE Transactions on Information Theory*, vol. 57, pp. 3530–3536, 2011 (https://doi.org/10.1109/TIT.2011.2143830).

Mar Mar Lwin, Student
School of Electrical and Electronic Engineering
https://orcid.org/0009-0009-3920-5197
E-mail: mar.mar.lwin@student.usm.my
Universiti Sains Malaysia, Nibong Tebal, Malaysia
https://www.eng.usm.my

Mohd Fadzli Mohd Salleh, Ph.D., Assoc. Professor
School of Electrical and Electronic Engineering
https://orcid.org/0000-0002-1801-6049
E-mail: fadzlisalleh@usm.my
Universiti Sains Malaysia, Nibong Tebal, Malaysia
https://www.eng.usm.my